

Placental contractions in uncomplicated pregnancies

Authors:

Louise Dewick^{1*}, Amy L Turnbull², Kate F Walker¹, Nia W Jones¹, George Hutchinson², Christopher Bradley², Taqwa Ferdous³, Aisha Razzaque³, Ruizhe Li⁴, Xin Chen⁴, Graziela Figueredo⁴, Craig Platt⁵, Cesar Peres⁵, Penny Gowland²

Affiliations

¹ Centre for Perinatal Research, University of Nottingham, Nottingham, UK

² Sir Peter Mansfield Imaging Centre, University of Nottingham, Nottingham, UK

³ Department of Obstetrics and Gynaecology, Nottingham University Hospitals NHS Trust, Nottingham, UK

⁴ School of Computer Science, University of Nottingham, Nottingham, UK

⁵ Department of Histopathology, Nottingham University Hospitals NHS Trust, Nottingham, UK

*Corresponding author

Email: louise.dewick@nottingham.ac.uk (LD)

LD and ALT are Joint Senior Authors

Abstract

We first described the utero-placental pump phenomenon, *in utero*, in 2020. We have recruited 36 healthy pregnant women to undergo magnetic resonance imaging (MRI) between 29 and 42 weeks of pregnancy to further explore this occurrence in a single centre prospective observational study. Participants had fetal ultrasound to confirm normal growth. Dynamic MRI was acquired for between 15 and 32 minutes using respiratory triggered, multi-slice, single shot, gradient echo, echo planar imaging covering the whole uterus. All participants had a live birth of a healthy baby weighing over the 10th centile for gestational age and no conditions associated with placental dysfunction e.g. pre-eclampsia. There were no cases of severe maternal or fetal villous malperfusion on placental histopathology.

Visible contractions were recorded for all participants who completed MRI scans. Contractions involving a decrease in placental volume >10% were classified as either placental or uterine by visual observation. Placental contractions occurred more frequently than uterine contractions ($p=0.0061$), were associated with a larger increase in the surface area of the uterine wall *not* covered by the placenta ($p=0.0015$), sphericity of the placenta ($p<0.0001$) and longer durations ($p=0.0151$). Contractions led to an increase in the MRI parameter R_2^* in the placenta. There was large variation both between participants and between contractions from the same individual,

in terms of the time course and features of contractions. Rate, duration and other features of contractions did not apparently change across the gestational age range studied, although the largest fractional volume changes were detected at early gestation.

We found that placental contractions occurred in at least 60% of our healthy pregnant population with a median frequency of 2 per hour and median duration of 2.4 minutes.

Introduction

A healthy placenta is key to a successful pregnancy outcome, but much remains unknown about the function of this vital organ. Compromised placental function can lead to morbidity and mortality for both the mother and baby. Antepartum stillbirth affects over 1 in 250 pregnant women in the UK each year (1), and estimates suggest approximately 35% of stillbirths are attributable to placental dysfunction (2). Methods to detect developing placental dysfunction in pregnancy are largely indirect and focused on the growth and activity levels of the fetus. However, ultrasound assessment of fetal growth may be inaccurate or falsely reassuring and maternal perception of fetal movements is subjective. This has led to a focus on finding new reliable methods to detect placental dysfunction.

In 2020, using magnetic resonance imaging (MRI) in pregnancy we uncovered a new physiological phenomenon: the placental contraction or ‘utero-placental pump’, where the placenta/placental bed contracts independently of the rest of the uterine wall. This was observed in both healthy pregnancies and those complicated by pre-eclampsia, and demonstrated an *in utero* physiological occurrence that scientists had hypothesised over for nearly a century (3).

As early as 1906, the term human placenta was noted to have smooth muscle cells in the chorionic plate (fetal side of the placenta, Figure 1), and in the early 1920s there was the first published hypothesis that the human placenta was capable of contraction (4). During the mid-1990’s Graf et al demonstrated that stem villi (often also called ‘anchoring villi’) contain myofibroblast cells, and that a second contractile system exists beyond the fetal blood system – termed the ‘extravascular contractile system’(5). Graf and his team confirmed that a perivascular sheath of contractile tissue surrounded each stem villi of the placenta, which they suggested could lead to whole placental contraction (6). They hypothesised that this interwoven network of extravascular contractile cells surrounding stem villi would likely play a role in both maternal and fetal haemodynamics, including the maintenance of venous return from the placenta (Figure 1).

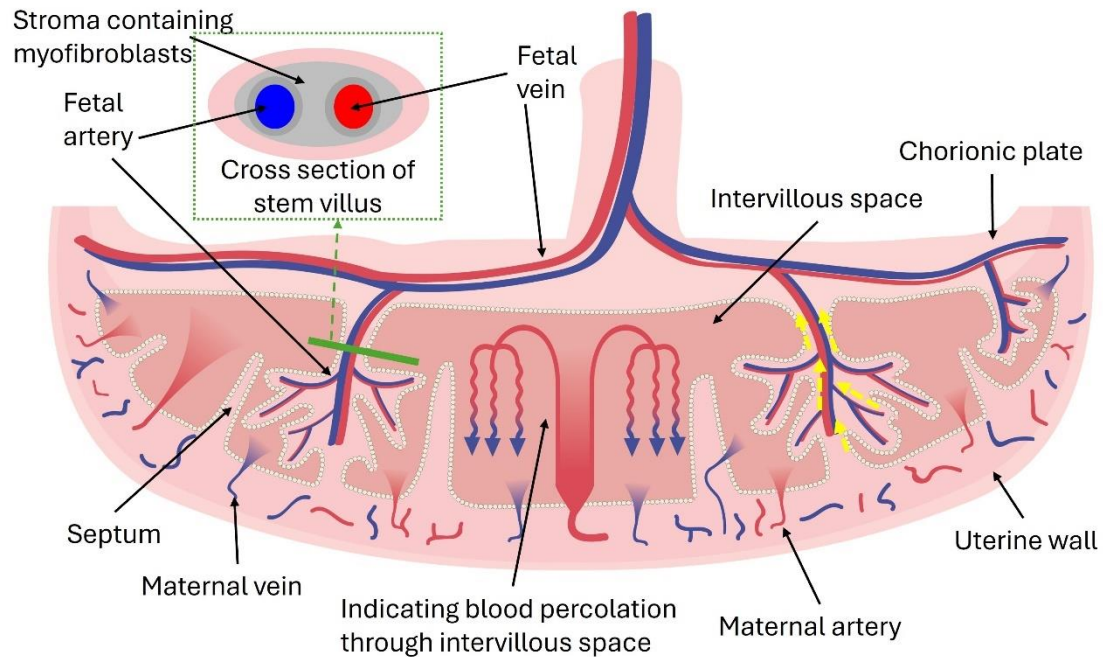


Fig 1. A schematic illustrating placental structure. Both arteries and veins contain smooth muscle in their vessel walls, but large stem villi (over 300µm), also contain myofibroblasts (smooth muscle cells) in the stroma surrounding the vessels, (termed Perivascular Contractile Sheath or Extravascular Contractile System). Stromal myofibroblasts are arranged parallel to the longitudinal axis of the stem villi and thus have the potential to induce longitudinal contraction (Demir 1997) (depicted by yellow dashed arrows), which could force blood out of the intervillous spaces via the maternal veins.

Subsequently, multiple researchers have reported that contraction of individual stem villi could reproducibly be achieved in the laboratory. Farley et al (7) dissected stem/anchoring villi from term placentae from uncomplicated pregnancies and demonstrated more than 40% increase in contractile tension in stem villi when exposed to potassium chloride, and 75% increase in contractile tension in stem villi when exposed to a nitric oxide synthetase antagonist L-NAME. To investigate the reversible nature of this phenomenon, they also exposed contracted villi to sodium nitroprusside and glyceryl trinitrate. These nitric oxide mimetics were capable of inducing stem villi relaxation of up to 74%, suggesting a potential role for nitric oxide in the regulation of stem villi contraction/relaxation and therefore materno-fetal blood flow.

Lecarpentier et al (8) used both potassium chloride and electrical tetanus stimulation to assess speed of shortening/contraction and tension in the stem villi. Interestingly, they demonstrated that the speed of stem villi contraction/shortening is the slowest currently known to occur in any mammalian organ, and 20 times slower than smooth muscle contraction in the human uterus. Kato et al(9) built a computational model of stem villi contraction, to demonstrate the likely haemodynamic impact and therefore purpose of this phenomenon, and demonstrated that stem villi contraction would displace both fetal and maternal circulations. This adds weight to the hypothesis of Farley and Lecarpentier that villous contraction is likely part of the maternal-fetal blood flow matching regulatory system present in human placentae.

However, work to date has been laboratory based, so the *in utero* significance of this placental contraction system remains theoretical. Dynamic MRI offers *in vivo* volumetric and haemodynamic measures with which to validate this *ex vivo* work. Echo Planar Imaging (EPI) is a very rapid MRI method that allows dynamic imaging of morphological changes in the placenta, which is R_2^* weighted. R_2^* (frequently referred to by its reciprocal T_2^*) is an MRI parameter that depends on multiple aspects of tissue structure, but in particular the concentration of deoxygenated blood. Placental R_2^* is known to increase in conditions associated with placental dysfunction and with gestational age (10-13), and has previously been reported to increase during contractions, but with no differentiation of placental and uterine contractions (14-17).

The aim of this study was to use MRI to demonstrate placental contractions in a healthy population and to characterise their magnitude, duration and frequency. Given prior clinical awareness of the existence of 'Braxton Hicks' uterine contractions, we attempted to classify the contractions visually as uterine or placental, and then measured basic morphological and MRI features of each type. This is a part of a larger multidisciplinary study with the goal of finding markers of placental stillbirth risk.

Methods

Ethics statement

Participants receiving antenatal care at Nottingham University Hospitals NHS Trust were recruited for the SWIRL (Stillbirth, When Is Risk Low?) study, and written, informed consent was obtained from each participant. The study was approved by the East Midlands–Leicester Central Research Ethics Committee (23/EM/0052).

Participant characteristics

Between 10th July 2023 and 29th February 2024, we recruited 36 women experiencing healthy, uncomplicated pregnancies to attend a single MRI scan between 29⁺⁰ and 42⁺⁶ weeks of pregnancy. As it was a pilot study, no formal sample size calculation was performed.

Inclusion criteria were singleton pregnancy, aged 18-50 years old, ability to give informed consent and the absence of risk factors for fetal growth restriction according to the Saving Babies Lives Care Bundle version 2(18). Exclusion criteria included women with a body mass index (BMI) of 45 kg/m² or over, claustrophobia, any contraindication to MRI scans, a baby with a lethal congenital abnormality and women without an ultrasonographic dating scan before 22 weeks' gestation.

All participants underwent an ultrasound assessment of fetal biometry, amniotic fluid volume, umbilical artery Doppler and uterine artery Doppler. To be considered low risk they needed to have an estimated fetal weight above the 10th centile for gestational age using Intergrowth 21 charts(19), an amniotic fluid index greater than 5cm and umbilical/uterine Dopplers under the 95th centile for gestation (20, 21). Clinical outcome data was collected retrospectively using the electronic patient record.

MRI

Participants were positioned at a lateral tilt, and scanned using a 3T Philips Ingenia MRI scanner, with one d-stream anterior body coil placed anterior to the participant and the

posterior bed coil. If, after localisers were performed and the location of the placenta was confirmed to be posterior and to have low signal to noise in that region, the participant was repositioned with the anterior body coil placed posterior to the participant (N=2 cases). Initially, multimodal MRI was performed to assess placental blood flow (data not reported here).

Dynamic MRI (a time course of multislice volume datasets) was then acquired for between 15 and 32 minutes, with the length of data acquisition depending on the mother's comfort.

Multislice volume datasets were acquired trans-axially to the mother, with the field of view covering the entire uterus. The sequence used was multi-slice, single shot, gradient echo, echo planar imaging (echo time 25ms, voxel size $1.56 \times 1.56 \times 6 \text{ mm}^3$, 32 slices, slice gap 4 mm, field of view $400 \times 400 \times 316 \text{ mm}$, Sense 3). The acquisition was respiratory triggered to expiration (trigger delay 200ms, minimum repetition time 9s, mean repetition time 15s).

A relatively large interslice spacing (10 mm) was used to achieve full coverage across the whole uterus in a relatively low number of slices; this interslice spacing has minimal effect on the accuracy of the volume estimates for these smooth objects. Full volume coverage was required to ensure that we accurately measured changes in placental and uterine volumes/areas, generally regardless of through plane motion between time points. Reducing the number of slices allowed us to limit the acquisition to the quiescent phase of the respiratory cycle, to ensure minimal motion through and between each volume, which simplifies segmentation of the uterus, placenta and fetus. Reduction in the number of slices acquired also reduced the acoustic burden on the mother and fetus. A slice gap (rather than increased slice thickness) was used to achieve this interslice spacing, to reduce slice cross talk due to movement and improve spatial resolution by reducing partial volume effects. The slices were acquired sequentially so that any residual motion between slices would be easier to interpret.

Data Analysis

Images were automatically segmented to estimate placental volume, fetal and fluid volume, placental bed area and remaining uterine wall (non-placental bed) area as shown in Figure 2. Segmentation was performed by nnU-Net(22) a convolutional neural network trained on 169 manually segmented volumes from 39 individuals. To evaluate segmentation performance, a 5-fold cross-validation at the subject level was conducted. The average Dice Coefficient across all volumes was 0.8134 ± 0.0560 for placenta and 0.9542 ± 0.0158 for the non-placental uterus. These results indicate good segmentation performance for both structures, with particularly high accuracy for the non-placental uterus.

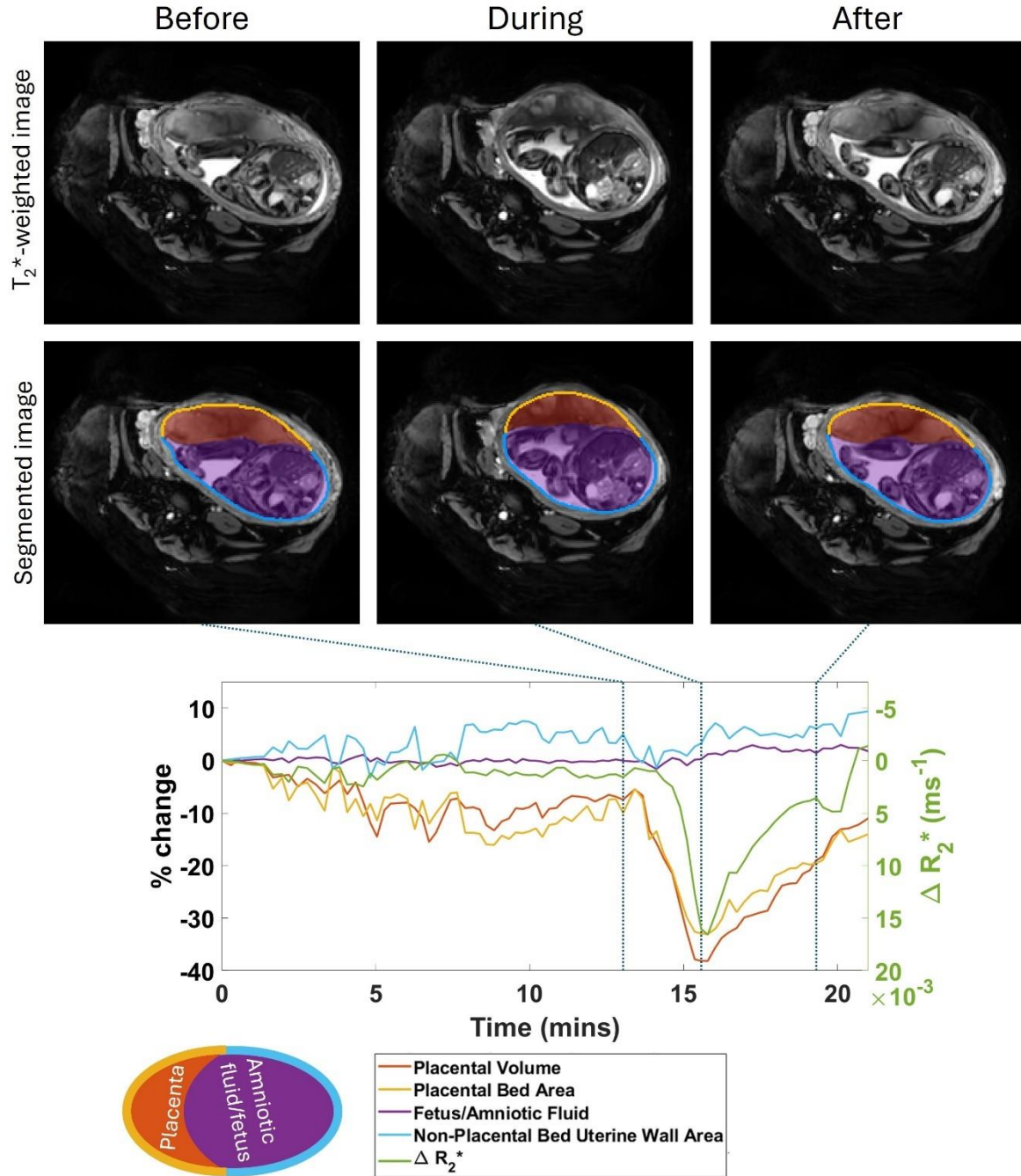


Fig 2: Uterine and placental changes during an example placental contraction. The top row shows axial MRI images at selected times points before, during and after a placental contraction (indicated by vertical lines on the graph below) with segmentations shown below. Changes in placental and non-placental volumes, wall areas and placental R_2^* (all measured across the whole volume of the uterus, not just the single slice shown) are plotted underneath. The legend indicates the colours used for the lines in the plots and the regions indicated in the segmentation.

The segmentations were used to create time courses of measured volumes and areas, with values normalised to the earliest rest volume (which was not the initial volume if the data acquisition started during a contraction). Time courses were smoothed using a moving average filter with a span of 5 timepoints. Placental sphericity was calculated using

$$Sphericity = \frac{\pi^{\frac{1}{3}}(6V)^{\frac{2}{3}}}{A}$$

where V is volume and A is surface area of the placenta. The change in R_2^* across the placenta mask was calculated using

$$\Delta R_2^* = -\frac{1}{TE} \ln\left(\frac{S}{S_0}\right)$$

where S is the average signal intensity in the placenta at each dynamic, S_0 is the value at the earliest rest volume and TE is the echo time.

The maximum percentage changes in volumes, areas and R_2^* were calculated during the contraction relative to baseline. This baseline was approximated as being linear between the value at the last rest volume before the contraction to the value at the first rest volume following it (vertical lines 1 and 3 on Figure 2). In cases where the start/end of a contraction occurred outside the scan duration, the baseline was assumed to be constant at the value at the end/start. Contractions were visually identified by inspecting both the cine series of dynamic images across multiple slices and plots of the changes in volume and area measurements together. After training and familiarization with the data (working with TF, AR and ND), two raters (PAG: 30 years' experience of placental MRI and ALT: 3 years' experience of placental MRI) identified contractions in all time courses, considering both the cine image time series (over multiple slices) and the volume/area time courses (Figure 3, and S1a and b). Both observers agreed on the occurrence of all contractions though they did not always agree on observed start and end times, particularly since the end could show an extended tail as the contraction relaxed (Figure 2). This did not affect the final results, as the duration of contraction was reported as the time between half maximum change in volume. The number of contractions detected was divided by the time over which data was acquired, to estimate the mean number detected per hour.

Given the previous knowledge that women experience uterine contractions or 'tightenings' during pregnancy, sometimes referred to as 'Braxton Hicks', two observers (PAG and ALT individually and then in consensus), classified contractions into two types based on dynamic morphological changes observed in the cine image time series and volume time courses (Figure 3).

- Placental contractions were defined as those generating an apparent shortening of the placental bed in the 2D images, an observed thinning of much of the non-placental bed section of the wall, and a change in placental shape particularly at the periphery of the placenta. Generally, the periphery of the placenta became more square and less tapered in profile and, if the apparent marginal sinus was visible, it usually disappeared.
- Uterine contractions showed little change in placental shape or size on the images, beyond sometimes becoming apparently thinner, with thickening of the uterine wall which could be either (a) local but not under the placenta (red arrows in Figure 3) or (b) uniform.

If both types of contraction were to occur simultaneously it is likely that they would be categorised as uterine by this process. We did this for all contractions but then separated out those with placental volume change $>10\%$, as consensus was sometimes difficult to achieve for smaller contractions.

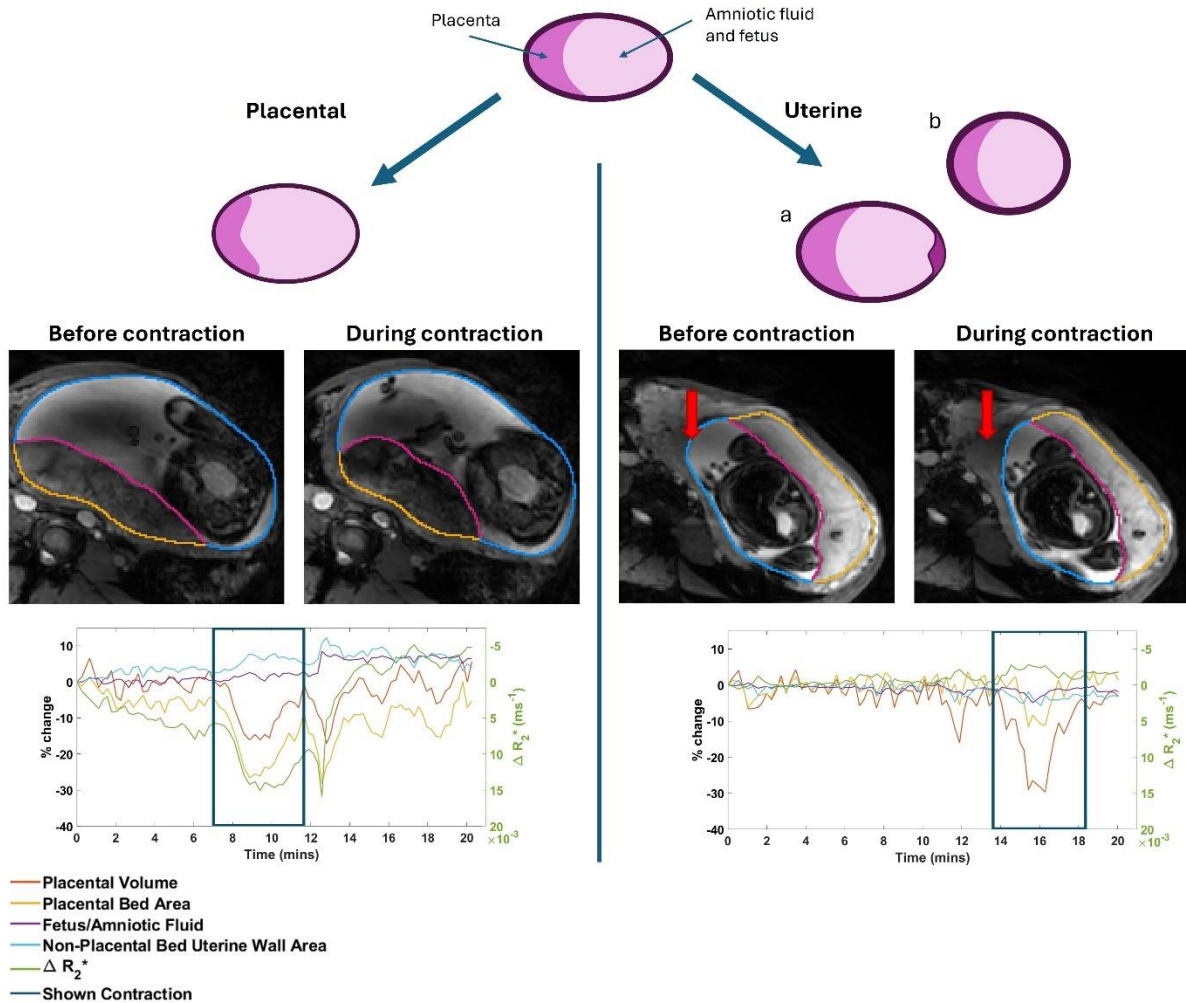


Fig 3: The morphological changes used to visually categorise placental and uterine contractions. Placental contractions are generally associated with an apparent shortening of the placental bed in the 2D images, a thinning of the wall not covered with the placenta, and a change in placental shape particularly at the periphery of the placenta. Uterine contractions are generally associated with little change in placental shape except some thinning, with thickening of the uterine wall that can be either (a) local (red arrows) or (b) uniform. The legend colours match figure 2 but regions are not shaded to improve visualization, so the pink line indicates the amniotic surface of the placenta. The plots show the changes in volumes, areas and signal with the example contraction highlighted. Both time courses show additional contractions with <10% placental volume change: LHS from 14.7-16.6 mins and 17.8 – 20.3 mins, RHS from 10.8 – 13.2 mins.

Statistical analysis

Differences between groups were compared using the Mann Whitney U test.

Results

Participant Demographics

The demographics of our cohort are shown in Table 1. All 36 women recruited were healthy with no chronic medical conditions known to impact fetal growth. One participant withdrew a few minutes into the scan due to feeling unwell and was removed from further analysis. Participants were all non-smokers, aged under 40 years old and had a first trimester BMI below 35kg/m². None of the participants developed any conditions associated with placental dysfunction e.g. fetal growth restriction, pregnancy induced hypertension or pre-eclampsia.

Table 1. Participant demographics

Variable	Category	n (% of whole cohort)
Maternal Age	18-24 years old	1 (3%)
	25-29 years old	4 (11%)
	30-34 years old	18 (51%)
	35-39 years old	12 (34%)
Maternal BMI ^a (first trimester)	<20 kg/m ²	1 (3%)
	20-24kg/m ²	15 (43%)
	25-29 kg/m ²	14 (40%)
	30-34 kg/m ²	5 (14%)
Primiparous		12 (34%)
Multiparous		23 (66%)
Previous miscarriages		11 (31%)
No previous miscarriages		24 (69%)
Ethnicity (self-reported)	White British	29 (82%)
	White European	3 (9%)
	Asian – Indian/Bangladeshi	2 (6%)
	Black African	1 (3%)

^aBMI, Body Mass Index;

Ultrasound assessment of fetal wellbeing

All fetuses in our cohort had umbilical artery and mean uterine artery pulsatility index values below the 95th centile for gestation at the time of their MRI scan. Their fetal growth and liquor volume measurements are shown in Table 2.

Table 2. Ultrasound assessment results to demonstrate fetal wellbeing

Variable	Category	n (% of whole cohort)
Estimated fetal weight centile	10 th -25 th	2 (6%)
	26 th -50 th	16 (46%)
	51 st -75 th	12 (34%)
	76 th - 99 th	5 (14%)
Amniotic Fluid Index	5 - 9.9cm	4 (11%)
	10 -14.9cm	20 (57%)
	15 -19.9cm	4 (11%)
	20 -25cm	3 (9%)
	unknown	4 (11%)

Birth outcomes

The mean gestation at birth was 279 days or 39 weeks and 6 days. The earliest birth was at 37 weeks and 1 day, and the latest birth was at 41 weeks and 5 days. There were no babies born preterm (< 37 weeks' gestation). Table 3 outlines the labour and birth outcomes: all babies in our cohort had normal Apgar scores, no evidence of intrapartum hypoxia and no evidence of significant placental dysfunction on histopathological examination.

Table 3. Labour and birth outcomes

Variable	Category	n (% of whole cohort)
Onset of labour	Spontaneous	19 (54%)
	Induced	9 (26%)
	No labour (elective caesarean)	7 (20%)
Mode of birth	Spontaneous vertex	16 (46%)
	Assisted/Instrumental	3 (9%)
	Elective Caesarean	7 (20%)
	Emergency Caesarean	9 (25%)

Fetal Sex	Male	15 (43%)
	Female	20 (57%)
Birthweight centile	<3rd centile	0 (0%)
	<10th centile	0 (0%)
	≥10th and ≤50th	8 (23%)
	>50 th and <90th	19 (54%)
	>90th centile	8 (23%)
5-minute Apgar score	<3	0 (0%)
	<7	0 (0%)
	>7	35 (100%)
Placental histopathology	Severe features of Maternal Arterial Malperfusion	0 (0%)
	Severe features of Fetal Villous Malperfusion	0 (0%)

Of the nine women who underwent induction of labour, five were induced due to reduced fetal movements at term, two had post-dates pregnancies, one had an unstable lie which became cephalic, and one participant had kidney stones requiring a nephrostomy. In the three women who underwent assisted vaginal/instrumental birth, the indication for one participant was delay in the second stage of labour, and for the other two there were fetal heart rate concerns. In the nine women who underwent emergency caesarean birth, one requested caesarean during labour, two had an unsuccessful induction of labour, three had delay in the first stage of labour, two had pathological fetal heart rate patterns and one had umbilical cord prolapse.

MRI

Contractions of the uterus/placenta were observed in all participants who completed scanning occurring at a rate of 6.3 (3.9,9.0) contractions per hour, with 8.4 (5.1,14)% placental volume decrease, 1.6 (1.1,2.2) minutes duration and R_2^* increase of 0.89 (-0.96,3.3) s^{-1} ; values reported

are (median (lower quartile ,upper quartile) in all cases. The variation in number of contractions across subjects is given in Figure 4a.

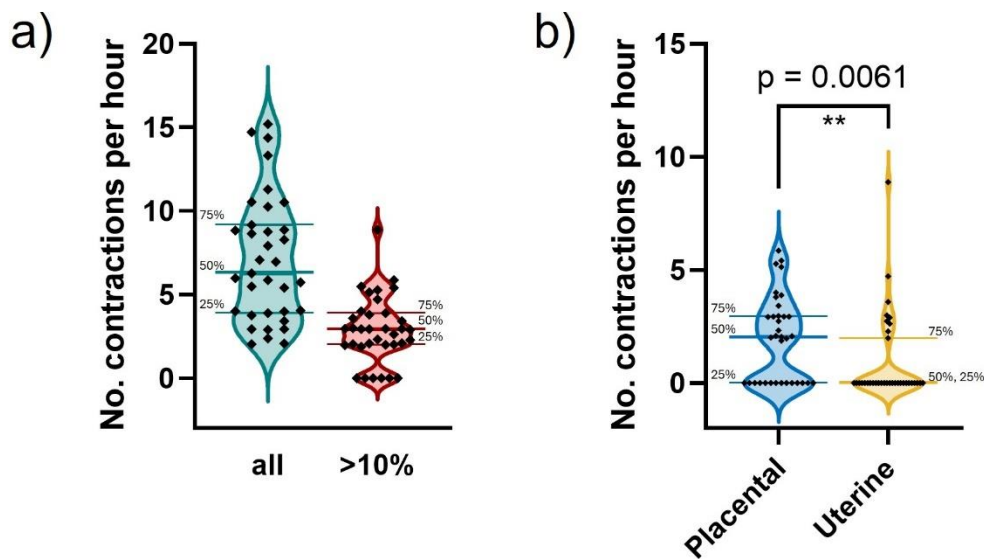


Fig 4: Number of contractions detected per hour (calculated from number detected divided by observation time). Median and interquartile values are marked. a: The left-hand bar shows this for all contractions; the right-hand bar shows it only for contractions with a placental volume change exceeding 10%. b: For placental and uterine contractions separately (with a placental volume change > 10% in both cases).

However, there was considerable variation; some subjects showed one deep, long contraction (35% volume decrease in Figure 2), whilst others showed bursts of smaller contractions (Figure 3).

Figure 4a shows that 41% of contractions showed a volume change >10%, and Figure 4b shows that these larger contractions were more likely to be classified as placental ($p=0.0061$). One contraction was removed from the analysis due to extensive whole maternal movement.

Figure 5 shows contractions defined visually as placental were associated with significantly greater increases in measured placental sphericity and non-placental bed uterine wall area than uterine contractions ($p < 0.0001$ and $p = 0.0015$ respectively), with uterine contractions often causing decreases in both these measurements.

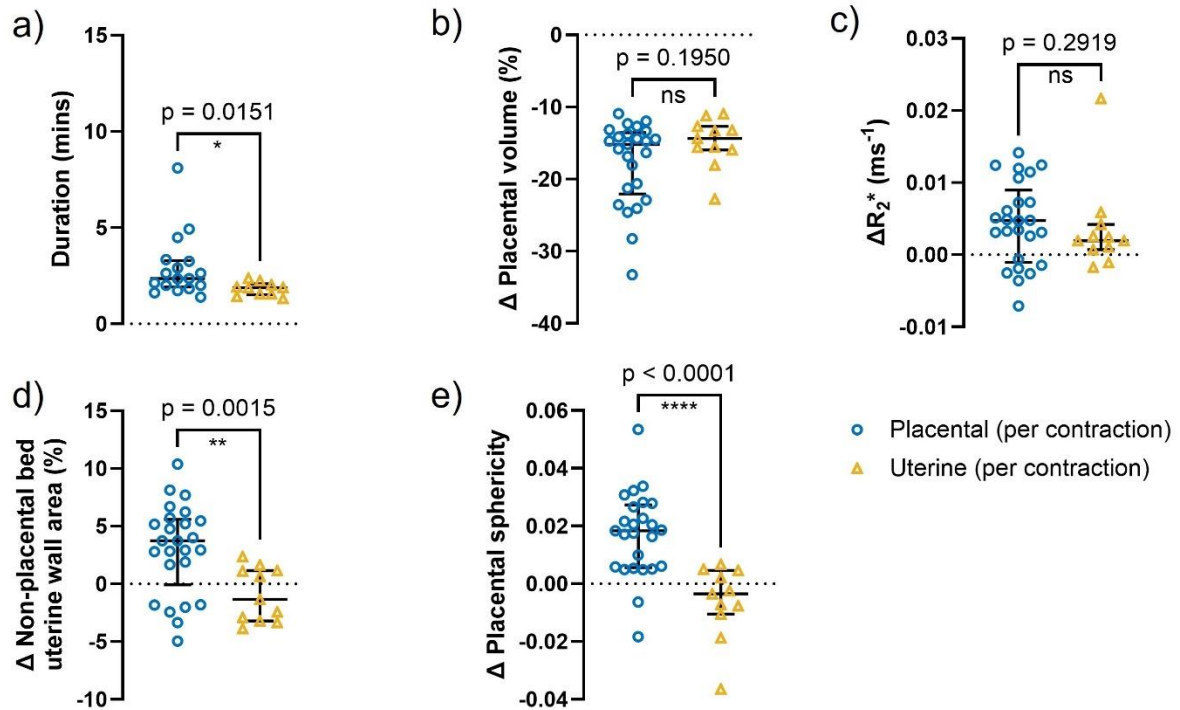


Fig 5: Characteristics of contractions with placental volume change >10%, shown separately for placental and uterine contractions. a) number of contractions per hour (calculated for varying scan times of 15-30 minutes), b) duration, c) ΔR_2^* and d) placental volume change. Median and interquartile range are shown for each group.

S2 Fig plots these parameters against each other. These results indicate that there are morphological differences between placental and uterine contractions (even for similar changes in net placental volume).

Placental contractions were also longer ($p=0.0151$) compared to uterine contractions. There was a non-significant trend for placental contractions to cause a larger increase in R_2^* and a trend for larger decrease in placental volume.

Figure 6 presents data for all contractions (not just those with >10% placental volume change) and shows that there was large variation both between participants and between contractions from the same individual in a given scan session. It also shows no apparent change with gestational age in the rate and duration of contractions, placental volume reduction and change in R_2^* ($p = 0.64, 0.27, 0.65$ and 0.56 respectively), although there was a trend for the largest %volume changes to occur in early gestation, perhaps reflecting the smaller absolute volume of the resting placenta at that stage of pregnancy.

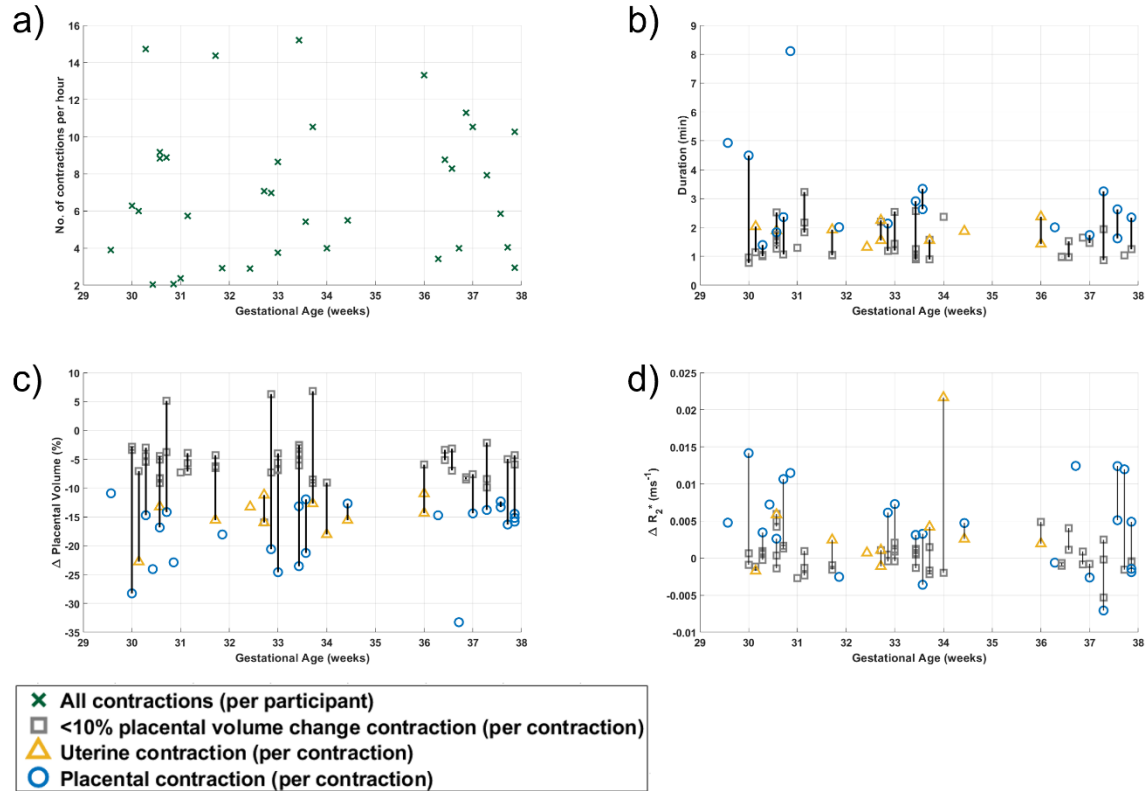


Fig 6 Variation in contraction features with gestational age for all contractions identified visually (including those with volume changes of less than 10%): a) rate of any contraction, b) duration, c) change in placental volume and d) change in R_2^* of all contractions across gestational age. Contraction type is shown by marker style and contractions from the same individual scan session are joined.

Discussion

All 35 participants showed placental or uterine contractions in the period for which they were studied, with 30 participants showing any contractions with $>10\%$ change in placental volume and 21 showing placental contractions above this threshold. The *in utero* observation of placental contractions confirms the hypothesis of placental contractions first made over a century ago and characterises the phenomenon of a ‘utero-placental pump’ previously identified by our group. The placental contractions observed during a single MRI session of 15-32 minutes varied in both rate and duration between participants. Placental contractions leading to a volume change $>10\%$ occurred at a median rate of two per hour but this figure does not fully characterise the timing of the contractions, which could occur singly or in a short burst. Longer data acquisition periods, perhaps with alternative detection mechanisms, are required to investigate the temporal distribution of contractions.

In this work contractions were detected and classified visually by two observers based on morphological features (Figure 3). This subjective approach was necessary given that there is no gold standard with which to compare. However, we also considered differences in quantitative metrics between the two types of contractions. All contractions were associated with a reduction in placental volume and although there was a trend for placental contractions to involve a larger decrease in volume (up to 35% in some cases), this difference was not

significant, although this may have been biased by only considering contractions with >10% placental volume change. Both placental and uterine contractions are expected to cause reductions in placental volume since both will increase the pressure in the uterine cavity. Hence, depending on resistance to maternal venous return, they will push blood out of the placenta and into the maternal veins, since the fetus and amniotic fluid are incompressible.

However, there were morphological differences between placental and uterine contractions. In particular, the area of the uterine wall not covered by the placental bed increased more in placental than uterine contractions ($p=0.0015$). If placental contractions only involve a reduction in the area of the placental bed, then they might be expected to frequently involve an increase in the rest of the uterine wall area, as the remaining wall still needs to cover the incompressible fetal and amniotic fluid volume. However, the extent of this increase will depend on the relative volume changes in the fetus/amniotic sac, placenta and areas of the placental bed as well as the rest of uterus.

Placental contractions also tended to be longer than uterine contractions ($p=0.0151$), with some being several minutes in duration. The contraction durations measured using MRI are defined based on the change in the volume of the placenta which is determined by both mechanical effects and the haemodynamics of the intervillous space and vessel refilling. It is likely that these durations cannot be compared directly to shorter durations measured by electrohysterogram (EHG) or mechanical movement of the body wall (detected by the pressure transducer in cardiotocography/CTG) for labour contractions. We defined length as the time between half maximum contraction points: the full length, from the start of contraction to the approximate point of complete refilling (which is not well defined - Figure 2) was 3.1 (2.3, 4.7) min (median and IQR). It is likely that the rate of refilling provides information about placental haemodynamics and is being investigated in future studies including compromised pregnancies.

Furthermore, placental sphericity increased significantly more for placental than uterine contractions ($p<0.0001$). This is probably because when the placenta contracts the placental bed area gets smaller so the placenta appears to get thicker (more spherical), whereas when the entire uterus contracts, the placenta tends to get thinner. During placental contractions there is a large reduction in the area of the placental bed (with no contraction of the rest of the uterus) so the placenta could be expected to “balloon” to support its volume. Contraction of the stem villi could limit this ballooning and hence ensure that placental contractions squeeze blood from the IVS into the maternal circulation. Alternatively, placental contractions are remarkably slow and as noted above, stem villus shortening *ex vivo* is known to be very slow, suggesting that contraction of the villi might trigger the placental bed area to contract. Direct imaging of the villous trees, probably combined with a mechanical and hydrodynamic model of the placenta might provide a way to test these competing hypotheses.

There was a non-significant trend for placental contractions to be associated with a larger change in placental R_2^* of up to 0.02 ms^{-1} . The increase in R_2^* during the contraction probably reflects a reduction in spiral artery flow leading to deoxygenation during the contraction as well as a change in the distribution of deoxygenated blood in the placenta, an increase in tissue density, and increased movement of blood in the placenta. However, no consistent change in absolute R_2^* was found between the start and end of a contraction, although this can be difficult to measure if scanning period does not cover one end of the contraction, or two contractions slightly overlap.

Some features used in visual designation of contractions overlap with the quantitative morphological features, but we have presented both for two reasons. First the quantitative metrics provide confidence that the visual, subjective categorization is indeed sensitive to shape changes that support the hypothesis that the placenta is contracting independently of the rest of the uterus.

Secondly these measures point the way to future automated categorization of contractions, for instance by thresholding the plot shown in Figure S2a. To be rigorous we did not revisit the final visual classification after comparison to the quantitative metrics, but it might be argued that any contraction associated with either a significant increase in non-placental wall area or increase in sphericity must be placental, based on the geometrical considerations, and expected nature of placental contractions described above. This is supported by the divergence of these metrics with increasing placental volume changes for placental and uterine contractions, shown in Figure S2 b) and c), as well as the apparent correlation between these measures and change in R_2^* (Figure S2 d) and e)) indicating that, while the change in placental volume during these contractions is comparable, the greatest impact on placental haemodynamics is seen when the placenta contracts and changes shape.

However, we are also investigating whether the visually sorted data can be used to train a machine learning algorithm for detecting and categorising different types of contractions.

Strengths and weaknesses of the study

In order to define how placental contractions contribute to placental physiology, this study investigated placental contractions in a cohort of women with structurally normal and clinically healthy placentas, as confirmed by the ultrasound data obtained during pregnancy, outcomes of labour and birth, and placental histopathology.

However, the study is weakened by its small sample size (35 pregnancies) which will have reduced our statistical power to detect differences in the features of contractions with gestational age or between placental and uterine contractions. In addition, 86% of the women studied were aged over 30 at the time of birth and the average age of our cohort was 32.4 years, whereas the national average age of a first birth is 30.9 years (1). This may reflect the higher proportion (63%) of multiparous women in our study, which was probably because we recruited women with healthy pregnancies, and having had a prior successful pregnancy confers a much lower risk of placental complications in subsequent pregnancies. Another weakness of this study is its low proportion of ethnic minorities. In the UK approximately 18% of the population are non-white and locally in Nottingham this rises to 34% (1). In our cohort only 3 of 35 participants self-reported their ethnicity as non-white, which makes our findings less generalisable to the wider population.

A further limitation of our study is the short duration of the dynamic MRI acquisition (15-32 minutes), limited by the need to ensure the study was acceptable to participants. This snapshot of placental function may not be generalisable over a longer time period, e.g. 24-48 hours, and did not allow contractions of both kinds to be seen in all cases, limiting the precision in the measured rate of contractions. Conventional MRI also limited us to studying placental contractions whilst women were lying laterally, which may not be representative of placental function in other positions or during exercise. In future we aim to investigate this using wearable devices.

In our previous work more women showed no obvious placental contractions during their MRI scan (3), but that is probably because that MRI acquisition was shorter. Furthermore, in the previous study only immediately obvious contractions were manually segmented, whereas in this study full data sets were automatically segmented so that the volume time course curves were available to assist in identifying any contractions. That study was also confounded by the use of hyperoxia in the protocol.

Considering technical aspects of this study, the whole volume of the uterus was scanned and segmented to detect placental contractions. This improves the precision of the volume and area time course curves and overcomes the risk of maternal breathing or movement altering the region being interrogated which might create an artificial change in the volume time courses that could be interpreted as a contraction. In R_2^* weighted MRI, an echo time given by $TE=1/R_2^*$ will provide maximum sensitivity to a change in R_2^* , and the TE used here was chosen to provide reasonable sensitivity across the range of baseline R_2^* values previously observed in healthy placentas. However, this work could benefit from optimizing the echo time per subject and possibly working at lower field strength where the R_2^* values will be shorter

It would be valuable to acquire simultaneous electrohysterography (EHG/EMG) and MRI data, although this is challenging since in an MRI scanner physiological abdominal motion induces artefactual signals in EMG data.

Meaning of the study: possible mechanisms and implications for clinicians

In our previous work, and in multiple prior studies concerning the contractile capabilities of placental stem villi, it has been hypothesised that the underlying purpose of this contractile mechanism is to influence maternal and fetal haemodynamics within the placenta.

This study confirms the occurrence of placental contractions in healthy pregnancy, and importantly found that placental contractions were very slow (with a median full duration of three minutes, which is much longer than uterine contractions in labour). This supports Lecarpentier's finding that stem villi show ultra-slow contraction velocity (8).

The underlying physiological significance of these slow placental contractions remains unclear. We did not observe a consistent change in R_2^* between the start and end of the contraction which might suggest there was no bulk change in oxygenation. However, this measurement was difficult because the ends of the contractions are hard to define and often merged into other events (e.g. other contractions, fetal movement, end of data acquisition etc). There was a significant change in R_2^* during the contraction, but this is to be expected if the inflow is reduced and tissue volume fraction is increased at this time. Further work will consider magnetic susceptibility changes from MRI (which are a more direct measure of oxygenation) and a larger population of women, to allow us to constrain measurements to contractions where the end is clearly defined.

An alternative function of the contractions could be to remove unstirred layers of blood, which are likely to form in the slow flow/low oxygen gradient regime of the intervillous spaces (3). This relates to the concept of placental 'materno-fetal blood flow matching'. There is general consensus that the placenta possesses an intrinsic mechanism to protect fetal blood flow from

large changes in blood flow direction or velocity occurring as a result of changes in maternal spiral artery flow into the intervillous spaces, for example during maternal movement. (23) Local materno-fetal blood flow matching can be achieved by redistribution of fetal villous blood flow (via vascular cuffs) in response to the oxygen level in the surrounding intervillous spaces (24, 25). Alternatively ultra-slow villous and placental bed contractions could provide a mechanism by which maternal blood flow in/out of the intervillous spaces is controlled in order to 'match' with fetal blood flow, to maximize oxygen uptake in a given time (7, 8) and is likely to lead to refreshment of blood across the entire IVS. This is likely to be more relevant when dealing with more global oxygenation mismatches. We are now using mathematical modelling to investigate how to optimize our R_2^* and magnetic susceptibility MRI scans to detect such changes.

Unanswered questions and future research

Questions remain regarding the physiological trigger and initiation of placental contractions given the lack of intrinsic pacemaker. In 2010 Suci et al(26) found telocyte cells in the placental stroma alongside stem villi perivascular contractile sheaths. These telocytes are already known to exist in other endocrine/contractile organs (the small intestine and pancreas). They proposed that these telocytes represent a co-ordinated network across the placenta which allows stem villi to contract in a co-ordinated fashion. Electrophysiological currents generated by telocytes (27) are capable of initiating smooth muscle contraction, for example in the myometrium of the uterus, but as the placenta is a non-innervated organ, other researchers have suggested that co-ordination of villi contraction may be direct cell to cell communication or via a paracrine mechanism (28). In this work, we have demonstrated that placental contractions are accompanied by a reduction in the placental bed area of the uterine wall, but we cannot directly observe the behaviour of the villi. However, if the stem villi and placental bed did not contract in concert, then it is likely that a reduction in placental bed area alone would be inefficient and would lead to a ballooning of the chorionic plate. As discussed above, future work could study the morphological changes in the placenta in more detail and in combination with a physical model, to try to determine whether the contraction originates in the wall or chorionic plate.

We now need to investigate whether placental contractions are altered in compromised pregnancies. In 2010 Khozhai et al(29) examined the difference in number of smooth muscle cells/myofibroblasts between healthy and compromised placentas, and found more extravascular stromal smooth muscle cells and thicker perivascular contractile sheaths in pre-eclamptic and growth restricted pregnancies. What remains unclear is whether the increase in extravascular contractile cell types is the result of placental dysfunction or whether it generates the haemodynamic changes which lead to placental dysfunction. Suci et al(26) hypothesised a link with placental pathology/insufficiency/remodelling as telocytes are known to express angiogenic vascular endothelial growth factor (VEGF), a biomarker whose role in pre-eclampsia is yet to be fully established. Bosco et al(28) reviewed the role of telocytes in co-ordinating stem villi contraction and therefore materno-fetal blood flow. They hypothesized that the oxidative stress resulting from maternal under-perfusion could reduce telocyte and therefore pacemaker function, which in turn could disrupt stem villi contraction and negatively impact oxygen and nutrient transfer across the intervillous space. However further work is required to understand the role of the contractions in healthy pregnancies and those compromised by conditions such as fetal growth restriction or pre-eclampsia.

Conclusion

This study extends our previous work, providing *in utero* evidence for placental contractions, which had previously only been hypothesized from *in vitro* studies.

These results will be valuable for designing further studies, and our segmentation algorithm can be shared to accelerate future work. These findings have informed the design of an ongoing longitudinal study into the characteristics of placental contractions in compromised pregnancies, through which we aim to establish if there are associations between the rate, duration or nature of placental contractions with other markers of placental or fetal wellbeing or with adverse pregnancy outcomes. Furthermore, we are developing a wearable device which will allow us to monitor placental contractions in varying maternal positions and over a longer time period to improve our understanding of this phenomenon.

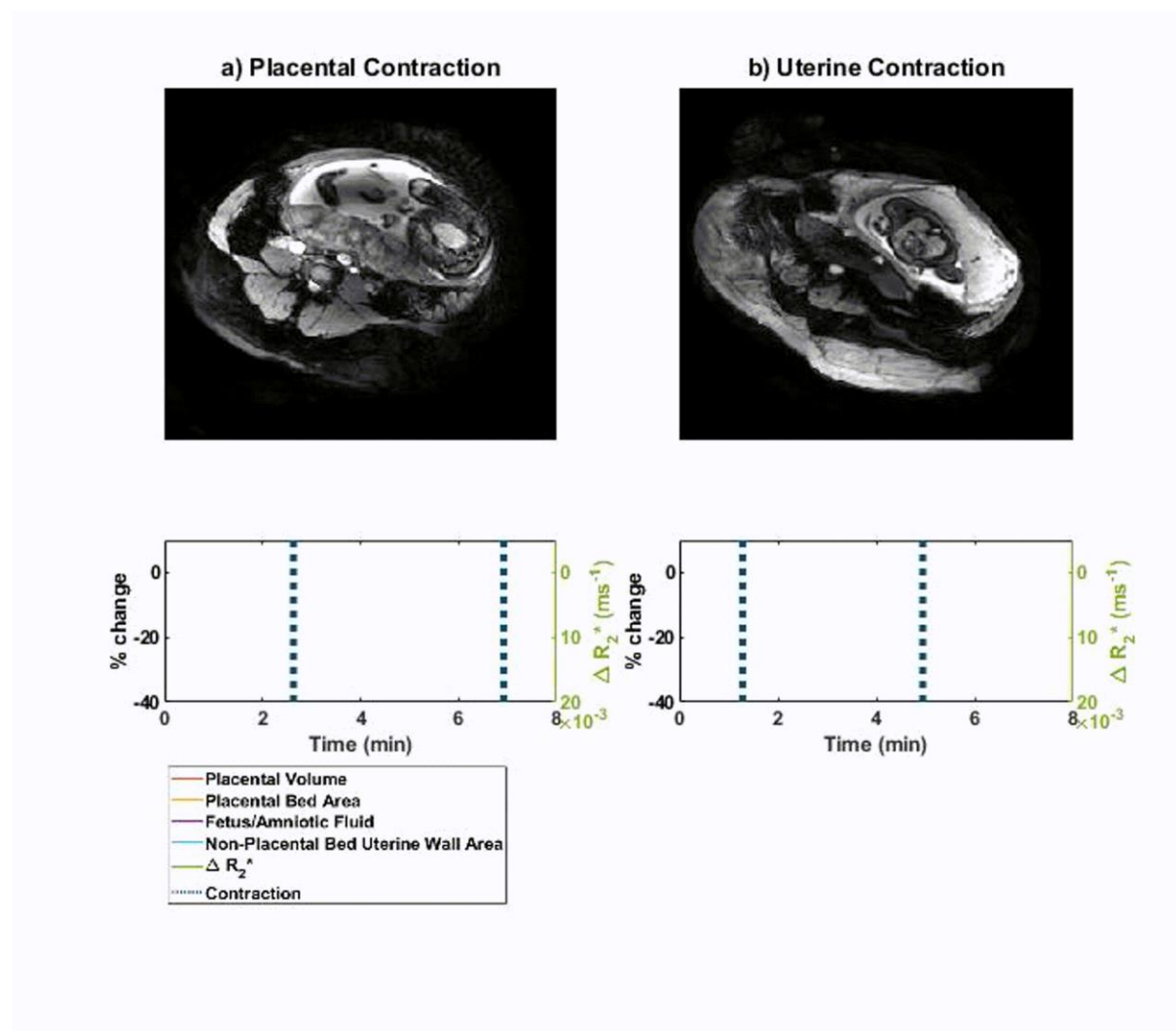
References

1. Census 2021: Office for National Statistics; 2021. Available from: <https://www.ons.gov.uk/peoplepopulationandcommunity/culturalidentity/ethnicity/bulletins/ethnicgroupenglandandwales/census2021>.
2. MBACE-UK. Perinatal Mortality Surveillance Report. NPEU, 2022 October 2022. Report No.
3. Dellschaft NS, Hutchinson G, Shah S, Jones NW, Bradley C, Leach L, et al. The haemodynamics of the human placenta in utero. *PLOS Biology*. 2020;18(5):e3000676. doi: 10.1371/journal.pbio.3000676.
4. KRANTZ KE, PARKER JC. CONTRACTILE PROPERTIES OF THE SMOOTH MUSCLE IN THE HUMAN PLACENTA. *Clinical Obstetrics and Gynecology*. 1963;6(1):26-38. PubMed PMID: 00003081-196303000-00003.
5. Graf R, Schonfelder G, Langer JU, Oney T, Reutter W, Schmidt H. The extravascular contractile system of the human placenta: A new aspect for the function of the organ?. [German]. *Zentralblatt fur Gynakologie*. 1994;116(6):344-6. PubMed PMID: 24201579.
6. Graf R, Schonfelder G, Muhlberger M, Gutschmann M. The perivascular contractile sheath of human placental stem villi: Its isolation and characterization. *Placenta*. 1995;16(1):57-66. doi: <https://dx.doi.org/10.1016/0143-4004%2895%2990081-0>. PubMed PMID: 25049963.
7. Farley AE, Graham CH, Smith GN. Contractile properties of human placental anchoring villi. *American Journal of Physiology-Regulatory, Integrative and Comparative Physiology*. 2004;287(3):R680-R5. doi: 10.1152/ajpregu.00222.2004. PubMed PMID: 15142834.
8. Lecarpentier Y, Claes V, Lecarpentier E, Guerin C, Hébert J-L, Arsalane A, et al. Ultraslow Myosin Molecular Motors of Placental Contractile Stem Villi in Humans. *PLOS ONE*. 2014;9(9):e108814. doi: 10.1371/journal.pone.0108814.
9. Kato Y. Influence of Branching Patterns and Active Contractions of the Villous Tree on Fetal and Maternal Blood Circulations in the Human Placenta. In: Aslanidis T, editor. *Highlights on Hemodynamics*. Rijeka: IntechOpen; 2018.
10. Sun Z, Wu W, Zhao P, Wang Q, Woodard PK, Nelson DM, et al. Association of intraplacental oxygenation patterns on dual-contrast MRI with placental abnormality and fetal brain oxygenation. *Ultrasound Obstet Gynecol*. 2023;61(2):215-23. Epub 20230112. doi: 10.1002/uog.24959. PubMed PMID: 35638228; PubMed Central PMCID: PMC9708928.
11. Gowland PA, Freeman A, Issa B, Boulby P, Duncan KR, Moore RJ, et al. In Vivo Relaxation Time Measurements in the Human Placenta Using Echo Planar Imaging at 0.5 T. *Magnetic Resonance Imaging*. 1998;16(3):241-7. doi: [https://doi.org/10.1016/S0730-725X\(97\)00308-1](https://doi.org/10.1016/S0730-725X(97)00308-1).

12. Zun Z, Kapse K, Quistorff J, Andescavage N, Gimovsky AC, Ahmadzia H, et al. Feasibility of QSM in the human placenta. *Magnetic Resonance in Medicine*. 2021;85(3):1272-81. doi: <https://doi.org/10.1002/mrm.28502>.
13. Sørensen A, Hutter J, Seed M, Grant PE, Gowland P. T2*-weighted placental MRI: basic research tool or emerging clinical test for placental dysfunction? *Ultrasound in Obstetrics & Gynecology*. 2020;55(3):293-302. doi: <https://doi.org/10.1002/uog.20855>.
14. Abaci Turk E, Stout JN, Feldman HA, Gagoski B, Zhou C, Tamen R, et al. Change in T2* measurements of placenta and fetal organs during Braxton Hicks contractions. *Placenta*. 2022;128:69-71. Epub 20220829. doi: 10.1016/j.placenta.2022.08.011. PubMed PMID: 36087451; PubMed Central PMCID: PMC9674925.
15. Sinding M, Peters DA, Frøkjær JB, Christiansen OB, Uldbjerg N, Sørensen A. Reduced placental oxygenation during subclinical uterine contractions as assessed by BOLD MRI. *Placenta*. 2016;39:16-20. doi: <https://doi.org/10.1016/j.placenta.2015.12.018>.
16. Hutter J, Kohli V, Dellschaft N, Uus A, Story L, Steinweg JK, et al. Dynamics of T2* and deformation in the placenta and myometrium during pre-labour contractions. *Sci Rep*. 2022;12(1):18542. Epub 20221103. doi: 10.1038/s41598-022-22008-3. PubMed PMID: 36329074; PubMed Central PMCID: PMC9633703.
17. Abaci Turk E, Abulnaga SM, Luo J, Stout JN, Feldman HA, Turk A, et al. Placental MRI: Effect of maternal position and uterine contractions on placental BOLD MRI measurements. *Placenta*. 2020;95:69-77. doi: <https://doi.org/10.1016/j.placenta.2020.04.008>.
18. England N. Saving Babies' Lives Care Bundle Version 3 2023 [cited 2023 27/10/2023]. Available from: <https://www.england.nhs.uk/long-read/saving-babies-lives-version-3/#element-2-fetal-growth-risk-assessment-surveillance-and-management>.
19. Papageorgiou AT, Ohuma EO, Altman DG, Todros T, Ismail LC, Lambert A, et al. International standards for fetal growth based on serial ultrasound measurements: the Fetal Growth Longitudinal Study of the INTERGROWTH-21st Project. *The Lancet*. 2014;384(9946):869-79. doi: 10.1016/S0140-6736(14)61490-2.
20. Ciobanu A, Wright A, Syngelaki A, Wright D, Akolekar R, Nicolaides KH. Fetal Medicine Foundation reference ranges for umbilical artery and middle cerebral artery pulsatility index and cerebroplacental ratio. *Ultrasound in Obstetrics & Gynecology*. 2019;53(4):465-72. doi: <https://doi.org/10.1002/uog.20157>.
21. Gómez O, Figueras F, Fernández S, Bennasar M, Martínez JM, Puerto B, et al. Reference ranges for uterine artery mean pulsatility index at 11–41 weeks of gestation. *Ultrasound in Obstetrics & Gynecology*. 2008;32(2):128-32. doi: <https://doi.org/10.1002/uog.5315>.
22. Isensee F, Jaeger PF, Kohl SAA, Petersen J, Maier-Hein KH. nnU-Net: a self-configuring method for deep learning-based biomedical image segmentation. *Nature Methods*. 2021;18(2):203-11. doi: 10.1038/s41592-020-01008-z.
23. Sebire NJ, Talbert DG. The dynamic placenta: a closer look at the pathophysiology of placental hemodynamics in uteroplacental compromise. *Ultrasound in Obstetrics & Gynecology*. 2001;18(6):557-61. doi: <https://doi.org/10.1046/j.0960-7692.2001.602.doc.x>.
24. Melbourne A, Aghwane R, Sokolska M, Owen D, Kendall G, Flouri D, et al. Separating fetal and maternal placenta circulations using multiparametric MRI. *Magn Reson Med*. 2019;81(1):350-61. Epub 20180921. doi: 10.1002/mrm.27406. PubMed PMID: 30239036; PubMed Central PMCID: PMC6282748.
25. Sebire NJ, Talbert D. The role of intraplacental vascular smooth muscle in the dynamic placenta: a conceptual framework for understanding uteroplacental disease. *Medical Hypotheses*. 2002;58(4):347-51. doi: <https://doi.org/10.1054/mehy.2001.1538>.
26. Suciu L, Popescu LM, Gherghiceanu M, Regalia T, Nicolescu MI, Hinescu ME, et al. Telocytes in Human Term Placenta: Morphology and Phenotype. *Cells Tissues Organs*. 2010;192(5):325-39. doi: 10.1159/000319467.

27. Cretoiu SM, Radu BM, Banciu A, Banciu DD, Cretoiu D, Ceafalan LC, et al. Isolated human uterine telocytes: immunocytochemistry and electrophysiology of T-type calcium channels. *Histochemistry and Cell Biology*. 2015;143(1):83-94. doi: 10.1007/s00418-014-1268-0.
28. Bosco C, Díaz E, Gutiérrez R, González J, Parra-Cordero M, Rodrigo R, et al. A putative role for telocytes in placental barrier impairment during preeclampsia. *Medical Hypotheses*. 2015;84(1):72-7. doi: <https://doi.org/10.1016/j.mehy.2014.11.019>.
29. Khozhai LI, Otellin VA, Pozharisskii KM, Pavlova NG. Expression of contractile proteins α -actin and myosin of smooth muscle cells and of type IV collagen in human placenta at placental insufficiency in III trimester of pregnancy. *Journal of Evolutionary Biochemistry and Physiology*. 2010;46(3):275-81. doi: 10.1134/S0022093010030075.

Supporting Information



S1: Dynamic MRI video of contractions: a) placental and b) uterine contraction with associated changes in volume/area measurements and ΔR_2^* of the placenta.

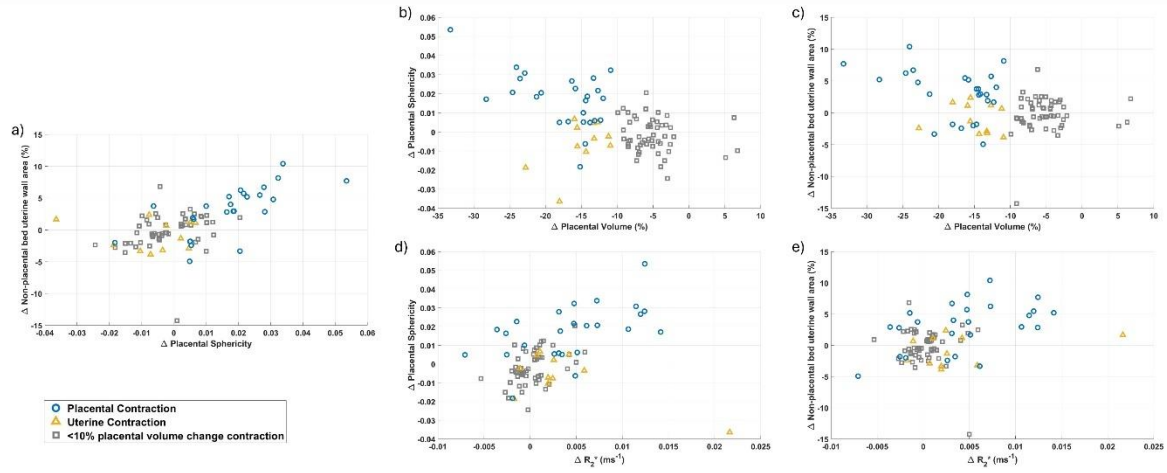


Fig S2: Relationship between change in placental sphericity and change in non-placental bed uterine wall area against contraction features per contraction, indicating morphological differences between contraction types. a) change in placental sphericity against change in non-placental bed uterine wall area, change in placental volume against b) change in placental sphericity and c) non-placental bed uterine wall area, change in R_2^* against d) change in placental sphericity and e) non-placental bed uterine wall area.